Polyimide-free homogeneous photoalignment induced by polymerisable liquid crystal containing cinnamate moiety

Rui He, Pushan Wen, Shin-Woong Kang, Seung Hee Lee & Myong-Hoon Lee

Polyimide-free homogeneous photoalignment induced by polymerisable liquid crystal containing cinnamate moiety

Rui He[a], Pushan Wen[a,b], Shin-Woong Kang[c], Seung Hee Lee[c,d] and Myong-Hoon Lee [a,d]

[a]Graduate School of Flexible and Printable Electronics, Chonbuk National University, Jeonju, Korea; [b]Department of Chemistry and Chemical Engineering, Zunyi Normal College, Zunyi, China; [c]Department of BIN convergence Technology, Chonbuk National University, Jeonju, Korea; [d]Department of Polymer-Nano Science and Technology, Chonbuk National University, Jeonju, Korea

ABSTRACT

We designed and synthesised a reactive mesogen (CRM) containing cinnamate moiety in the core and two acrylate groups at both ends. The structure was characterised by ^{1}H NMR and FT-IR, and its liquid crystalline property was investigated by DSC and POM. The compound showed a nematic phase between 175.2 – 97.5 °C, followed by a smectic C phase between 97.5 and 57.9 °C during the cooling cycle. We proposed a fabrication method to achieve uniaxial homogeneous alignment of liquid crystals by irradiating the CRM-doped LC mixture in a sandwich cell of in-plane switching mode (CRM-IPS) with linearly polarised ultraviolet light. The results indicated that the CRM-IPS cell showed excellent initial dark state with a good alignment state, electro-optical performance and durability. This confirmed that the photo-induced alignment of LCs by CRM possesses outstanding alignment capability compared to the conventional rubbed polyimide alignment layer. We expect that this fabrication method is a promising candidate for cost-effective, green-manufacturing, and high-quality alignment method for the manufacturing of high-resolution liquid crystal displays (LCDs).
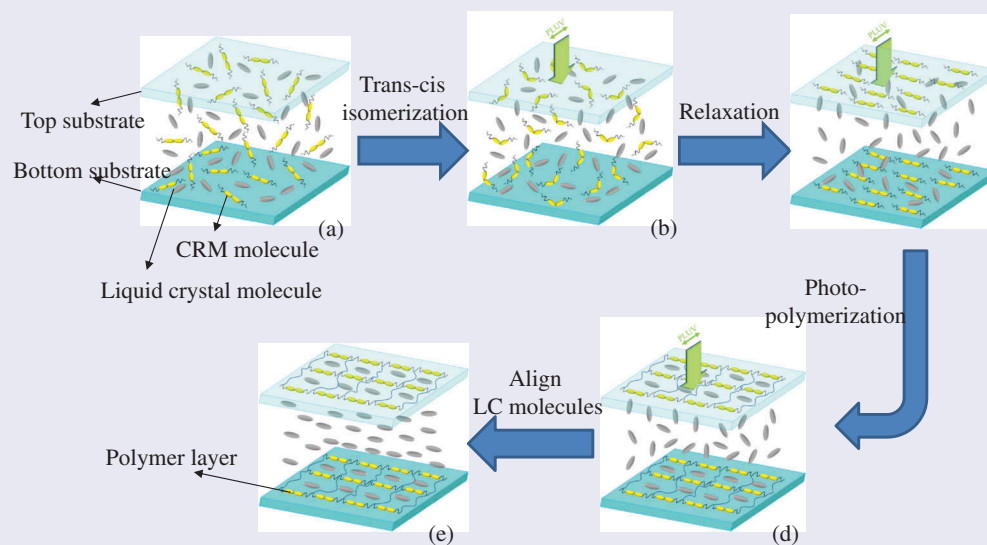
1. Introduction

Liquid crystals (LCs) have drawn much attention due to their unique state of matter. LC science and its applications now permeate almost all segments of the society from display industry to individual life. The liquid crystal displays (LCDs) are one of the most developed and dominated displays in the market due to its lightweight, low power consumption, low price, high resolution and so on [1]. Recently, the image quality of LCDs is rapidly improved with the adoption of several LCD modes such as multi-domain vertical alignment (VA) [2,3], in-plane switching (IPS) [4,5] and fringe-field switching (FFS) [6–12]. Among these developed LCD modes, the IPS and FFS mode LCDs are widely used in televisions,

monitors and smartphones due to the advantages such as wide viewing angle, fast response time and high transmittance. The high-performance of IPS and FFS LCDs is mainly attributed to the in-plane rotation of LC molecules [13]. One of the most crucial elements of these developed LCDs is the alignment layer, which is used for uniform homogeneous alignment of LCs at the surface. Various alignment techniques have been applied to achieve a uniaxial homogeneous alignment of LCs such as rubbing [14,15], ion beam alignment [16,17] and photoalignment [18–20] techniques. The rubbing technique is regarded as the industry standard technique to achieve a homogeneous alignment of LCs, because it produces the most reliable alignment for LCDs. However, the mechanical rubbing technique requires complicated processes of coating and high-temperature baking of polyimide layer as well as mechanical rubbing, which can result in some serious drawbacks such as debris generation, electrostatic charges and contamination problems [21]. Therefore, the alignment methods avoiding a mechanical contact with aligning surfaces have been actively studied [22–24]. One of the most promising alternatives for rubbing is the photoalignment technique, with which a uniformly homogeneous LC alignment can be achieved by irradiating linearly polarised ultraviolet (LPUV) light on a photosensitive alignment layer [25–29]. Nevertheless, photoalignment methods usually require processes such as film coating, baking, and UV irradiation with long processing time, which results in high cost and energy waste. Currently, to simplify the complex fabrication process and to achieve low-cost, efficient method in homogeneous LC alignment, several new approaches of photoalignment have been proposed [30–33]. Mizusaki et al. recently proposed a novel homogeneous alignment method without using conventional PI-layer in FFS cells. Thin polymer alignment layer was produced by photopolymerisation of a chalcone-based monomer mixed in the LC layer at above T_{NI} of the LC material. The FFS cell fabricated from this alignment method showed considerable alignment property and electro-optical properties [34]. The cinnamic functional group is well known for exhibiting a photo-induced isomerisation upon the LPUV exposure, which can be used for inducing a surface anisotropy to achieve alignment of LCs [20,35,36]. For example, Schadt et al. successfully created an alignment layer for LCD by irradiating LPUV on a spin-coated layer of poly(vinyl-*p*-methoxycinnamate) [20].

Based on these research results, we designed and synthesised a reactive mesogen compound containing a photosensitive cinnamate moiety in the core and two polymerisable acrylate groups at both ends (CRM). We investigated a homogeneous photoalignment method by irradiating the CRM-doped LC mixture in a sandwich cell with LPUV. Firstly, the synthesised compound (CRM) possessed a good compatibility with the host LCs due to its liquid crystalline property. Upon exposure with LPUV, a phase separation between the CRM and LCs formed an anisotropic polymer layer on the inner surface of substrates [32,37]. By this approach, we were able to fabricate a homogeneously aligned IPS cell (CRM-IPS) without using a conventional alignment layer. In this work, we describe the synthesis and characterisation of the CRM, the fabrication processes of the CRM-IPS cell and its electro-optical properties. We believe that this simple fabrication method is one of the potential alternatives to the conventional alignment technique to achieve a low-cost, eco-friendly and effective alignment in LCDs.

2. Experimental

2.1. Materials

Ethyl 4-hydroxybenzoate, 6-chlorohexanol, acryloyl chloride, N,N-dimethylaniline, hydroquinone, toluene-4-sulphonic acid, 3,4-dihydro-2H-pyran, 4-dimethylaminopyridine (DMAP), N,N'-dicyclohexylcarbodiimide (DCC), pyridinium toluene-4-sulphonate (PPTS), 4-hydroxycinnamic acid, N,N-dimethylphenol, 2,6-di-tert-butyl-4-methylphenol, 2-butanone, diethyl ether, dichloromethane, ethanol, 1,4-dioxane were purchased from Sigma-Aldrich and used without further purification. NaI, NaOH, KOH, HCl were purchased from TCI. The LC material (VA-J70) of negative dielectric anisotropy with T_{NI} = 74.5°C, $\Delta\varepsilon$ = −3.2, Δn = 0.109 was purchased from Merck.

2.2. Synthesis of CRM

The synthetic route of the liquid crystalline monomer having a cinnamoyl group (CRM) is demonstrated in Scheme 1.

2.2.1. Synthesis of 4-hydroxyphenyl 4-(6-acryloyloxyhexyloxy)benzoate (6)

The compound (3) and (4) were synthesised according to the reported procedure [38] and [39], respectively. To a 150 mL one-neck round bottom flask, were added 5.847 g (20 mmol) of compound (3), 3.885g (20 mmol) of compound (4), 0.244g (2 mmol) of 4-dimethylaminopyridine (DMAP) and 55 mL of dichloromethane. The mixture was stirred in an ice bath, and 4.54 g
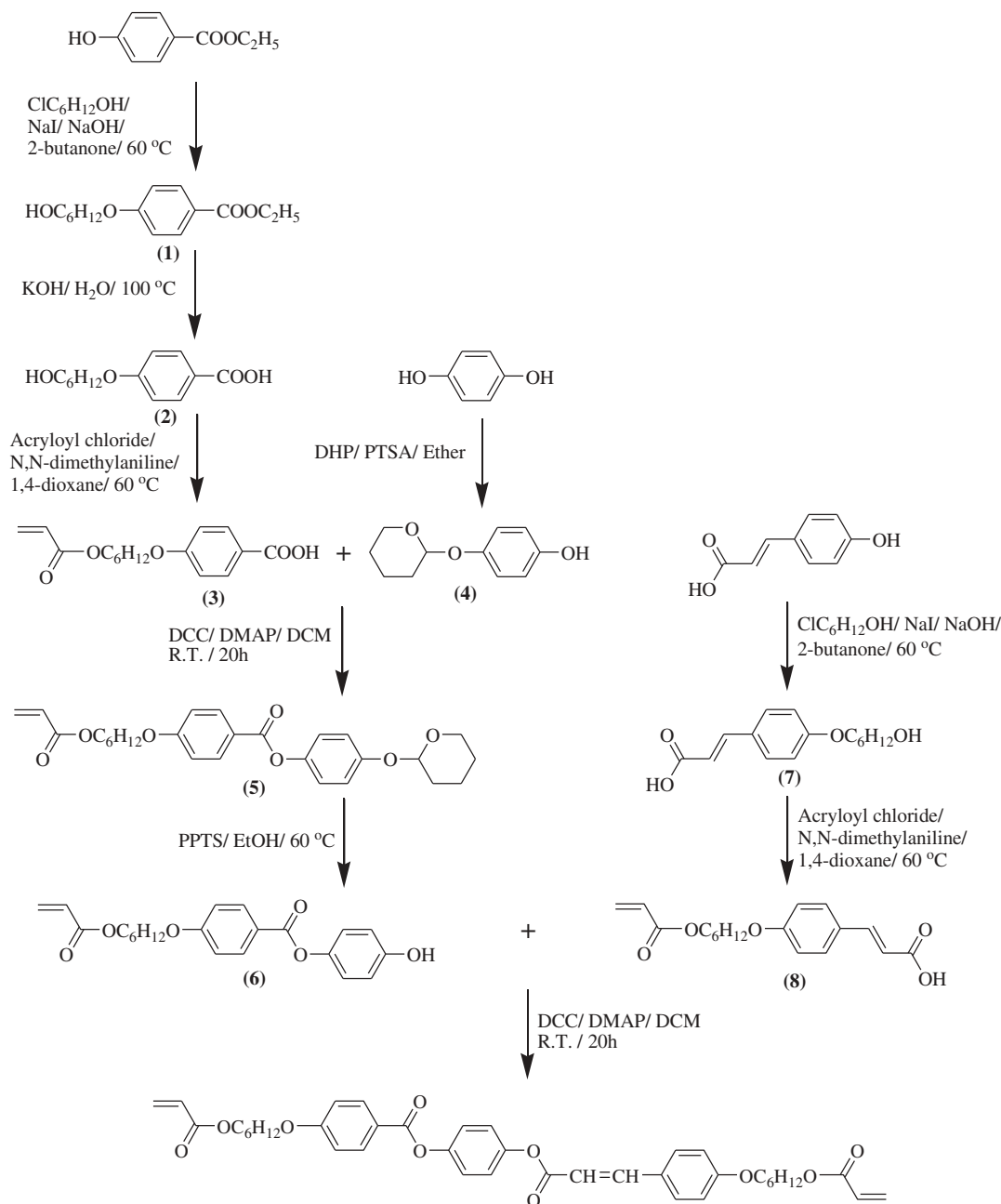
Scheme 1. Synthetic route for CRM.

(22 mmol) of N,N'-dicyclohexylcarbodiimide (DCC) was added with stirring. After stirring for 20 h at room temperature, the mixture was filtered through a pad of silica gel, and the solvent was evaporated to obtain the crude compound (5) as a clear oil that solidified on standing overnight. This crude product was recrystallised from ethanol to obtain compound (5) as white solid. Compound (5) was mixed with 0.251 g of (1 mmol) pyridinium toluene-4-sulphonate (PPTS) dissolved in 50 mL of ethanol. The mixture was heated at 60°C for 4 h until a clear solution was obtained. The solution was poured into 180 g of ice/

water mixture to obtain a white precipitate. The precipitate was filtered, washed with water and dried in a vacuum oven to obtain compound (6) as a white powder. Yield: 75%.

2.2.2. Synthesis of 4-(6-hydroxyhexyloxy)cinnamic acid (7)

To a 50 mL one-neck round bottom flask, 1.642 g (10 mmol) of 4-hydroxycinnamic acid was dissolved in 15 mL of ethanol. To this, 1.683 g (30 mmol) of KOH and 0.166 g (1 mmol) of KI dissolved in 5mL of water were added dropwise. The mixture was heated at

80°C for 10 min, and then, 1.708 g (12 mmol) of 6-chlorohexanol was added dropwise. After stirring for 48 h at 80°C, the solution was poured into water and extracted with diethyl ether. The aqueous layer was collected and neutralised with dilute aq. HCl until the solution became weakly acidic. The precipitated crude product was filtered, washed twice with water and dried in a vacuum oven. The crude product was recrystallised from ethanol to obtain compound (7) as a white powder. Yield: 67%.

2.2.3. Synthesis of 4-(6-acryloyloxyhexyloxy) cinnamic acid (8)

To a 50 mL one-neck round bottom flask, 1.586 g (6 mmol) of compound (7) and 0.873 g (7.2 mmol) of N,N-dimethylphenol were dissolved in 15 mL of 1,4-dioxane, and a trace of 2,6-di-*tert*-butyl-4-methylphenol was added to avoid unwanted thermal polymerisation. The solution was heated to 65°C with stirring, and 0.732 g (7.2 mmol) of acryloyl chloride was added dropwise. The solution was heated at 65°C for 3 h. After cooling, the solution was poured into water. The precipitate was filtered, washed twice with water and dried in a vacuum oven. The crude product was recrystallised from ethanol to obtain compound (8) as a white powder. Yield: 64%.

2.2.4. Synthesis of 4-(6-acryloyloxyhexyloxy) benzoyloxy 4-(6 acryloyloxyhexyloxy)cinnamate (CRM)

To a 50 mL one-neck round bottom flask, 1.154g (3 mmol) of compound (6), 0.955 g (3 mmol) of compound (8) and 0.0367g (0.3 mmol) of 4-dimethylamino-pyridine (DMAP) were mixed in 25 mL of dichloromethane. The mixture was stirred in an ice bath, and 0.680 g (3.3 mol) of N,N'-dicyclohexylcarbo-diimide (DCC) was added with stirring. After stirring for 20 h at room temperature, the mixture was filtered, and the solvent was evaporated to obtain white solid. The crude product was purified by chromatography (ethyl acetate: dichloromethane: petroleum ether = 1:5:10) to obtain pure CRM as a white powder. Yield: 76%.

2.3. Fabrication of IPS cells

2.3.1. Preparation of CRM-doped LC mixture

The LC material (VA-J70, Merck) and CRM were mixed in a weight ratio of 99: 1. The CRM/LC mixture was kept in ultrasonic bath at 75°C for 5 min and stored in an oven at 95°C for 30 min to assure a complete mixing.

2.3.2. Fabrication of CRM-ITO cell

At first, the cell was fabricated by assembling two ITO-glass substrates (CRM-ITO). The cell gap was maintained at approximately 5.0 μm. The CRM-doped LC mixture was injected into the plain ITO-cell by a capillary force at 95°C. Then, CRM-ITO cell was exposed with LPUV for a certain period of time at 95 °C with intensity of 5 mW cm^{-2} at 365 nm.

2.3.3. Fabrication of CRM-IPS cell

CRM-IPS cell was fabricated by combining a bottom IPS-substrate and a top bare glass substrate. The IPS-substrate was comprised of one-domain interdigitated electrodes with a pixel electrode (W = 7.0 μm) and a common electrode (L = 10.0 μm). The cell gap was maintained at approximately 5.0 μm. The CRM-doped LC mixture was injected into the CRM-IPS cell by a capillary force at 95°C. Then, the CRM-IPS cell was exposed with LPUV for 4 min at 95 °C with intensity of 5 mW cm^{-2} at 365 nm. The UV light was incident normal to the substrate, and the polarisation direction was set at 10º with respect to the electrode direction. The fabrication process of CRM-IPS cell is schematically illustrated in Figure 1.

2.3.4. Fabrication of PI-IPS cell

To compare electro-optical properties of the photo-aligned CRM-IPS cell with those of conventional IPS cell, we also fabricated an IPS cell with rubbed poly-imide alignment layers (PI-IPS). For rubbing-induced homogeneous alignment, both the IPS substrate (bottom) and bare glass substrate (top) were spin-coated with polyimide AL-16470 (JSR Co.), and uniaxially rubbed with a velvet cloth. The rubbing direction was set to 80° with respect to the electrode direction. Subsequently, top and bottom substrates were assembled antiparallel to the rubbing direction with 5 μm cell gap. The LC material (VA-J70, Merck) without CRM was injected into the PI-IPS cell by a capillary force at 95°C.

2.4. Measurements

The ^{1}H NMR spectrum of the CRM was recorded with JNM-AL400 FT/NMR spectrometers (400MHz, JEOL Ltd., Japan) in chloroform-d or DMSO-d$_6$ solvent. Fourier transform infrared spectroscopy (FT-IR) spectrum was obtained with a KBr pellet by using Shimadzu IR Tracer-100 spectrophotometer (Shimadzu Corp., Japan). Thermal decomposition property was investigated with TGA Q50 thermogravimetric analyser (TGA) (TA Instruments Inc., USA) at a heating rate of 10°C min^{-1} under nitrogen atmosphere. Differential
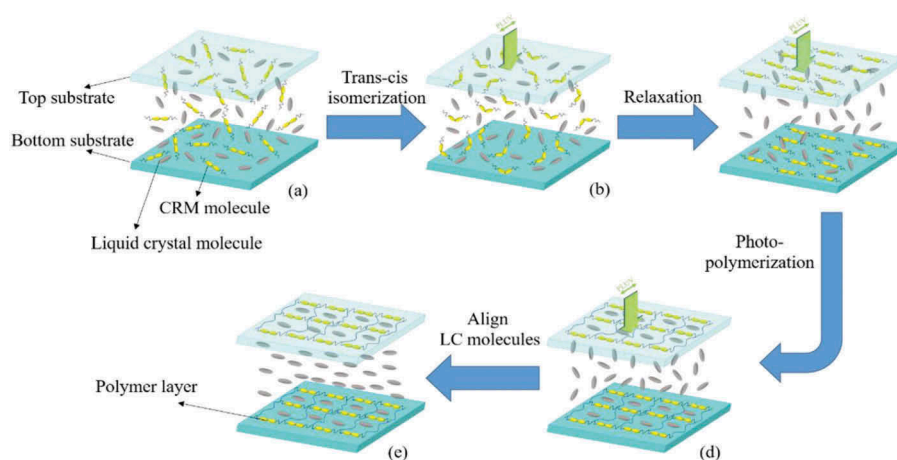
Figure 1. (Colour online) Schematic representation of fabrication process to achieve homogeneous alignment of LC.

scanning calorimetry (DSC) was conducted on DSC 2010 differential scanning calorimeter (TA Instruments Inc., USA) at heating and cooling rates of 5°C min^{-1} under nitrogen atmosphere. The phase transition behaviors of CRM were investigated by using a polarised optical microscope (POM, Nikon ECLIPSE LV100, Japan) equipped with Nikon DS-Ri1 digital camera. Polarised UV-Vis spectra were taken with the UV-Vis spectrophotometer (S-3100, Scinco Co., Korea). The inner surface images of the substrates were investigated by the field emission scanning electron microscopy (FE-SEM) (S-4300SE, Hitachi High-Technology Co., Japan). The pretilt angle of CRM-IPS and PI-IPS cells were measured with PAMS-200 (Sesim Photonics Technology Inc., Korea) pretilt measurement system. The electro-optical property and response time of CRM-IPS and PI-IPS cells were measured with LCMS-200 (Sesim Photonics Technology Inc., Korea) electro-optical evaluation system.

3. Results and discussion

3.1. Synthesis and characterisation of CRM

The CRM was synthesised according to the Scheme 1, and the synthetic procedures are described in the experimental section. The structure of the resulting CRM was characterised by ^{1}H NMR (Figure S1) and FT-IR (Figure S2) spectroscopic methods.

3.2. Phase transitions of CRM

The phase transition of liquid crystalline CRM was investigated by DSC (Figure 2) and polarised optical microscope (POM, insets in Figure 2). As shown in DSC curve, the CRM showed a smectic C phase between 86.8–102.6 °C and a nematic phase between

102.6 and 177.4 °C during the heating process. During the cooling process, a nematic phase appeared between 175.2 and 97.5 °C, followed by a smectic C phase between 97.5 and 57.9 °C. The phase transition behavior of CRM was also confirmed by the POM images during the cooling process. As shown in Figure 2, Figure 2(a) taken at 140 °C corresponds to the flow induced planar orientation of nematic phase in a thin cell. Figure 2(b) demonstrates the typical fan-shaped texture of smectic C phase at 95 °C. When cooled to 50°C, a crystalline phase was observed as shown in Figure 2(c). The results confirmed that the CRM is a thermotropic LC with wide mesomorphic temperature range.

3.3. Photo-induced alignment of CRM-IPS cell

Figure 1 illustrates the formation of photo-induced homogeneous alignment in a sandwich cell. The CRM-doped LC mixture was injected into the sandwich cell without a PI alignment layer. The CRM showed a good compatibility with the host LC material due to its liquid crystalline nature as observed by POM. The cell was irradiated by LPUV at 95°C, which is above the T_{NI} of host LC to avoid depolarisation of incident LPUV caused by birefringence of LC material. We speculated the mechanism of photo-induced homogeneous alignment as follows: Upon the absorption of LPUV, the liquid crystalline CRM containing cinnamic group undergoes a *trans-cis* photoisomerisation, with which *trans* forms having a molecular axis parallel to the polarised light are more rapidly isomerised to *cis* forms [35]. With continuing the LPUV irradiation at 95°C, *cis* forms are converted to *trans* forms by a thermal relaxation with the molecular axis either perpendicular or parallel to the incident polarised light. This results in
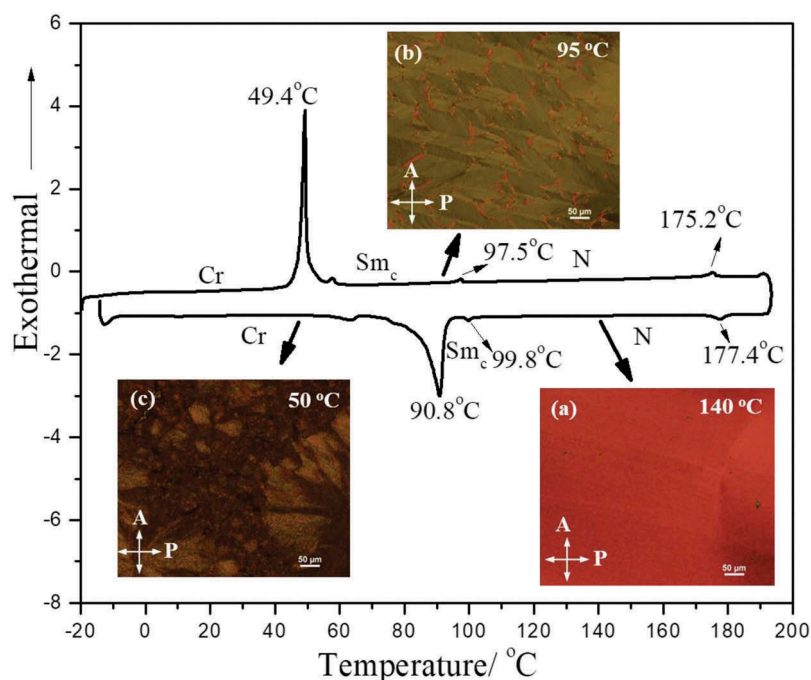
Figure 2. (Colour online) DSC thermogram and phase transition behavior of CRM. Insets are POM images representing (a) nematic phase at 140 °C, (b) smectic C phase at 95 °C and (c) crystalline phase at 50 °C.
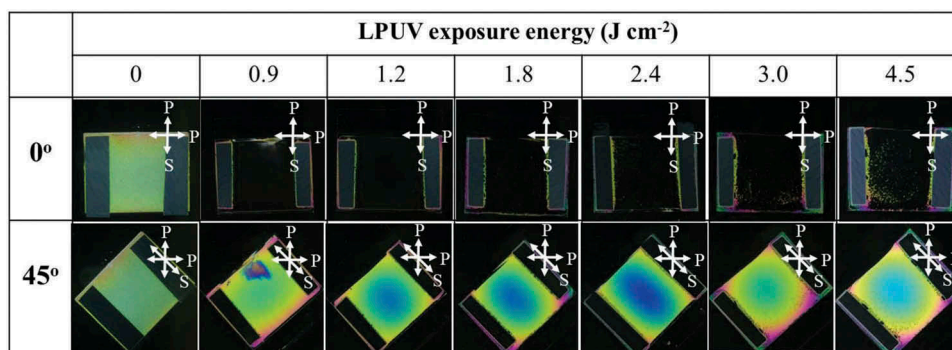

Figure 3. (Colour online) Photographic images of dark and bright states of CRM-ITO cells with various LPUV exposure energy.

the continuous reorientation of molecular axes of *trans* forms preferentially perpendicular to the incident LPUV. Meanwhile, a phase separation between the CRM and host LC occurs probably due to the formation of CRM oligomer, which causes the CRM to be deposited on the substrate surface with the formation of an anisotropic polymer layer. The anisotropic polymer layer is further fixed by photopolymerisation of acrylate groups [32,37]. When cooled down to room temperature, the LC molecules in the bulk are homogeneously aligned by the interaction with the anisotropic polymer layer surface. However, more extensive investigations should be necessary in the future to understand the detailed mechanism of photo-induced homogeneous alignment.

In order to find a homogeneous alignment condition, the LPUV exposure energy was varied in the range from 0 to 4.5 J cm^{-2}. Figure 3 shows the photographic images of dark and bright states of the CRM-ITO cell after LPUV irradiation with varying exposure energy. If the exposure energy is sufficient ($\geq$ 1.2 J cm^{-2}), the photographic images show completely dark and bright states under crossed polarizer when the alignment direction is 0° and 45° to the polarizer, respectively, which confirms the LC molecules are uniformly aligned on the ITO surface. When the exposure energy is less than 1.2 J cm^{-2}, the images show irregular bright and dark regions, indicating that LC molecules are not uniformly aligned. On the other hand, when the exposure energy is higher than 2.4 J cm^{-2}, the

CRM-ITO cells show some defects with partially disordered regions. This is probably due to the [2 + 2] photodimerisation between cinnamic moieties which could deteriorate the alignment quality of the polymer film formed on the substrates. Therefore, we selected the LPUV exposure energy to be 1.2 J cm^{-2} to achieve a high-quality homogeneous alignment in the further experiments.

To confirm the host LC molecules are oriented perpendicular to the electric vector of the incident LPUV, the top and bottom substrates were detached carefully and washed with hexane to remove the host LC. The top and bottom substrates were reassembled with 5 μm cell gap, and then, the LC mixture containing 1.0 wt.% of dichroic dye (disperse red 1) was injected to the cell at above the T_{NI}. It is noteworthy that the reassembled cell shows a dichroic absorption of visible light due to the aligned dichroic dye molecules by the 'host-guest' effect between the dichroic dye and aligned host LC molecules. This result indicates that the polymer layer on the substrates is stable and persistent. The polar diagram shown in Figure 4 was obtained from polarised UV-Vis absorption spectra of the cell containing dichroic dye and LC mixture as a function of azimuthal rotation angle. The maximum absorption observed at 90° indicates that the host LC molecules are oriented perpendicular to the electric vector of the incident LPUV. This result supports the previously speculated mechanism. The order parameter values were also estimated from the angle-dependent polarised UV-Vis spectra with different exposure energy, and the result is displayed in

Figure S4. The order parameter showed a maximum value at 1.2–1.8 J cm^{-2} and slightly decreased at higher exposure energy probably due to the reason explained above. From the above results, it can be concluded that the highest order parameter is obtained at the exposure energy of 1.2–1.8 J cm^{-2}, which is much lower than the reported value (5.0 J cm^{-2}) in the previous literature [32]. We suppose the higher sensitivity of our system is mainly attributed to the liquid crystalline nature of CRM, which could accelerate the rate of phase separation from the LC host when the *trans-cis* photoisomerisation occurs.

In order to further confirm the formation of the polymer layer on the substrates after LPUV exposure, the inner surface of the ITO cell was investigated with scanning electron microscopy (SEM) as shown in Figure 5, after detaching the cell and washing the top and bottom substrates with hexane. The cross-sectional image in Figure 5(a) and the surface view in Figure 5(b) indicate that a thin polymer layer was formed on both substrates with a thickness of around 50 nm.

3.4. Electro-optical properties of CRM-IPS and PI-IPS cells

The CRM-IPS cells were fabricated by using the photoinduced alignment process as mentioned above. Figure 6(a–c) show the POM images of CRM-IPS cell before and after LPUV exposure. Before LPUV irradiation, Figure 6(a) shows a typical nematic texture representing a random planar orientation. After LPUV
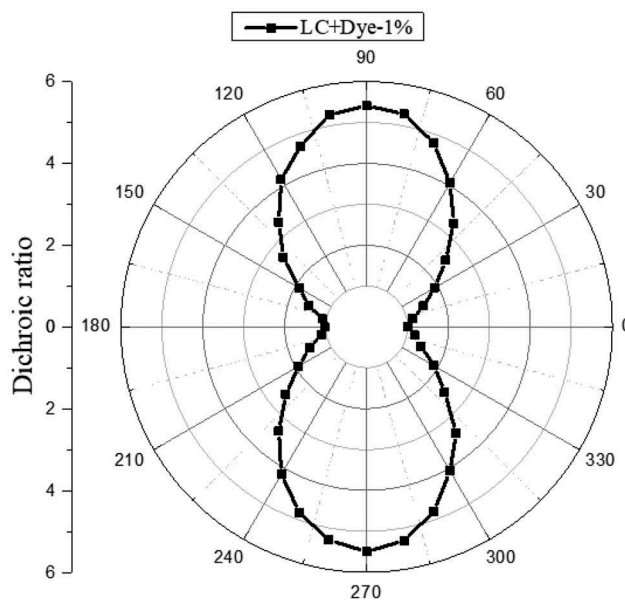

Figure 4. Angle-dependent polar diagram of dichroic ratio for reassembled CRM-ITO cell containing dichroic dye and LC mixture.
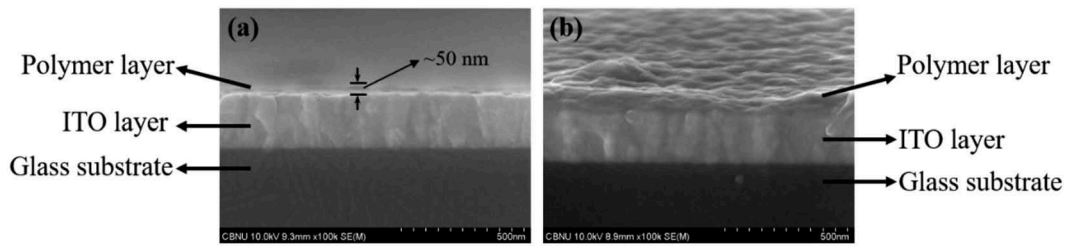
Figure 5. (Colour online) SEM images of substrate surface after LPUV exposure. (a) cross sectional view and (b) tilted view.
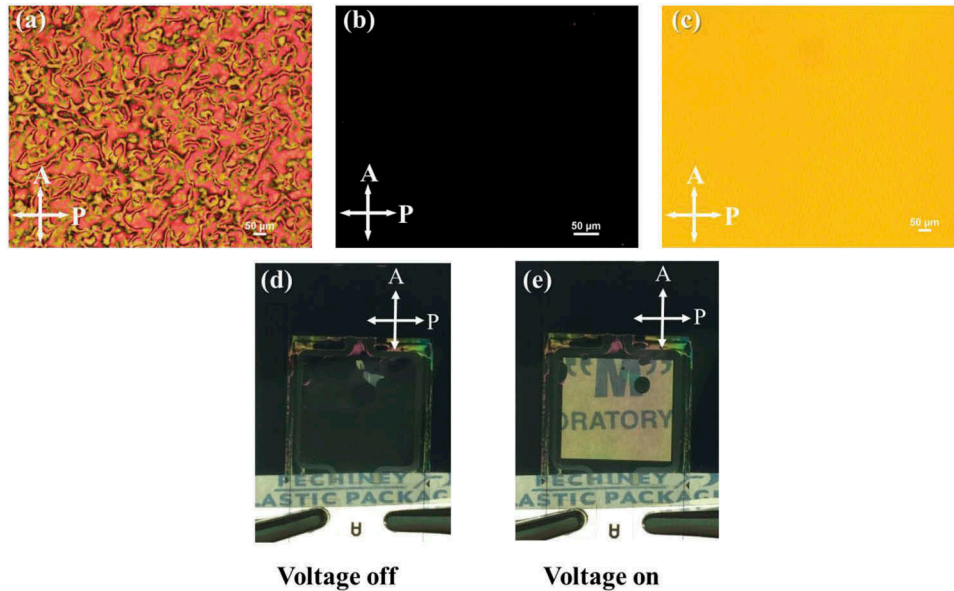

Figure 6. (Colour online) POM image of CRM-IPS cell (a) before UV exposure, (b) after UV exposure (LPUV axis is parallel to the analyzer direction) and (c) after UV exposure (LPUV axis is 45 $^{\circ}$ to the analyzer direction). Photographic image of CRM-IPS cell at (d) voltage-off state and (e) voltage-on state.

exposure at 95°C, a completely dark state (Figure 6(b)) and a bright state (Figure 6(c)) were observed with the LPUV direction parallel and 45° to the analyzer direction, respectively. Figure 6(d) and (e) show the photographic images of optical switching for the CRM-IPS cell at voltage off (0 V) and on states (8.8 V), respectively. The results indicated that uniaxial homogeneous alignment of LCs was achieved by this photoalignment process, and the resulting CRM-IPS cell possessed a decent electro-optical switching property. To further confirm the homogeneous alignment of LCs, the pretilt angles of the CRM-IPS cell were measured and compared with that of the conventional rubbed PI alignment cell (PI-IPS). The pretilt angles of the CRM-IPS cell and PI-IPS cell were 0.26° and 0.31°, respectively, which confirms that the CRM-IPS cell possesses homogeneous alignment state comparable to the conventional PI-IPS cell. To compare the electro-optical switching behavior of the CRM-IPS cell to the conventional PI-IPS cell, we obtained voltage-dependent

transmittance (V-T) curves of both cells under the same measurement condition. As shown in Figure 7, the V-T curves of CRM-IPS and PI-IPS cells are almost identical, indicating that the alignment capabilities of CRM photoalignment layer and the conventional rubbed PI layer are at the same level. In Figure 7, the inset images are the POM images of CRM-IPS and PI-IPS cells at voltage off (0 V) and on states (8.8 V), respectively. In both cases, the transmittance increased with increasing applied voltage from 0 to 9.0 V, and the gray-scales of both cells are almost at the same level. More detailed results are also shown in Figure S5. Moreover, the voltage-dependent response time of CRM-IPS and PI-IPS cells were measured at various applied voltages as shown in Figure S6. The rise time (τ_r) of CRM-IPS and PI-IPS cells were 64.0 and 64.1 ms, and the decay time (τ_d) of CRM-IPS and PI-IPS cells were 36.1 and 35.1 ms, respectively. There is no significant difference in the response time of CRM-IPS cell and PI-IPS cell. These results further
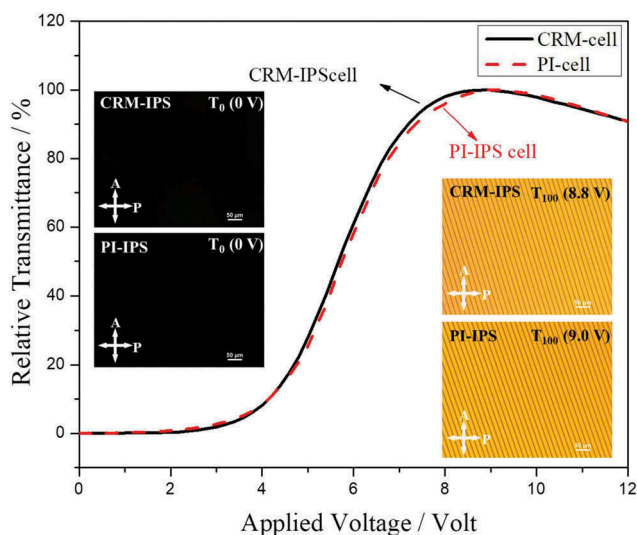
Figure 7. (Colour online) Comparison of V-T curves for CRM-IPS and PI-IPS cells. Inset images are POM images observed at voltage-off and voltage-on states, respectively.

Figure 8. (Colour online) V-T curves of CRM-IPS cell before and after voltage stress.

confirmed that the electro-optical switching properties of CRM-IPS cell are comparable to the conventional PI-IPS cell.

To compare the dark states quantitatively, we captured the dark state images of both the CRM-IPS and PI-IPS cells, and then, calculated the average brightness values by image processing. The light leakage values of CRM-IPS and PI-IPS cells are 0.436 and 0.465, respectively. The light leakage of CRM-IPS was 6.2% lower than that of the conventional IPS cell, indicating a better dark state for CRM-IPS cell. We assume that the higher light leakage of PI-IPS cell is possibly due to the debris or defects generated from the velvet cloth rubbing process. In addition, intrinsic perfect matching of alignment directions of the top and bottom substrates in the CRM-IPS cell could also be responsible for the better dark state. The single photoirradiation process automatically results in a perfect alignment matching of optical axes of the top and bottom substrates in the CRM-IPS cell. On the other hand, misalignment of optical axes is always unavoidable in the case of the PI-IPS due to the manual attachment of top and bottom substrates after the rubbing, which should result in a light leakage in the dark state.

3.5. Stabilities of photoaligned CRM-IPS cell

In order to test the anchoring energy of the CRM-IPS cell, AC field stress was performed by applying 60 Hz square wave with the applying voltage of V_{100} (8.8V) for 24 h at room temperature (V_{100} was defined as the
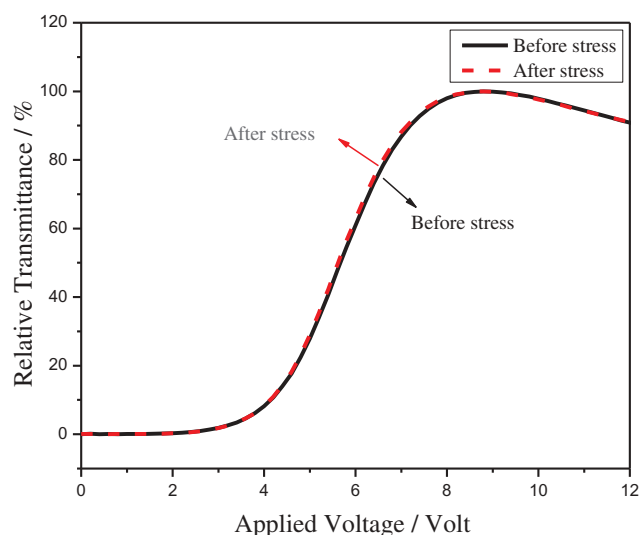
voltage which exhibits the maximum transmittance) to the CRM-IPS cell. Figure 8 compares the V-T curves of the CRM-IPS cell before and after voltage stress test. There is no any noticeable degradation can be observed in the V-T curves before and after the voltage stress, indicating a considerable anchoring stability of the photoaligned CRM-IPS cell.

Generally, the image quality and the reliability of LCD are not only depending on the electro-optical properties such as the response time and anchoring energy but also related to the durability of the cell. For the photoalignment technology, durability such as UV and thermal stability are crucial factors to achieve high-performance display with high image quality and long lifetime. For the thermal stability test, the cells were kept in 80°C chamber for 25 days, and the light leakage of the cell was measured with respect to the treatment time (Figure 9(a)). Similarly, for the UV stability test, the cell was irradiated with UV light of 10 mW/cm² (@365 nm) for 1 h, and the light leakage was measured with various exposure energy (Figure 9(b)). The alignment state and light leakage of each cell did not change significantly after the thermal or UV treatment. Additionally, the V-T curve of the CRM-IPS cell was measured before and after a consecutive process in which the CRM-IPS cell was first irradiated with UV light of 10 mW/cm² (@365 nm) for 1 h, and then, stored at 80°C for 25 days (shown in Figure 9(c)). As clearly seen, there was no substantial change in the electro-optical property even after the harsh UV and thermal stability test. These results illustrated that the
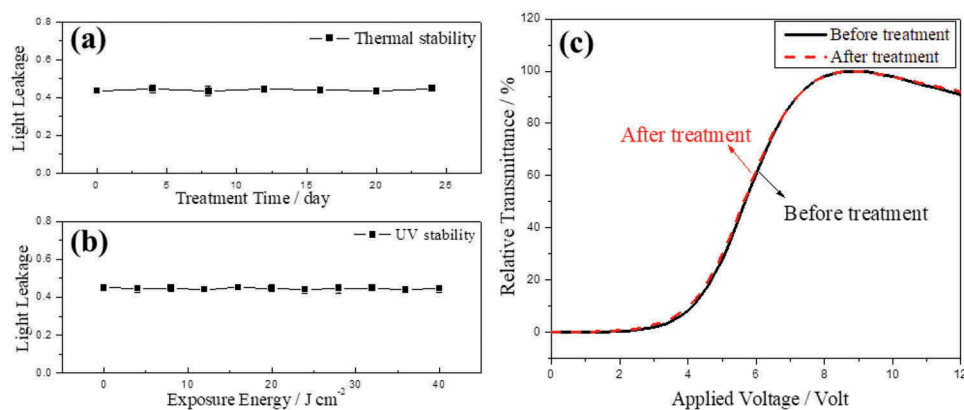
Figure 9. (Colour online) Durability of CRM-IPS cell. Light leakage of cells (a) after thermal treatment and (b) after UV treatment. (c) V-T curves of CRM-IPS cell before and after consecutive stability test.

homogeneously photoaligned CRM-IPS cell possesses a considerable stability for high-performance LCD application.

4. Conclusions

In this work, we synthesised a reactive mesogen (CRM) containing photo-sensitive cinnamic moiety in the mesogenic core and polymerisable acrylate groups at both ends. The resulting CRM was doped into conventional nematic LC, and the CRM-doped LC mixture was injected into a sandwiched cell with no alignment layers. After the irradiation of linearly polarised UV light at 95°C, a uniaxial homogeneous alignment of LC was achieved. Compared to the conventional LC cell with rubbed polyimide alignment layers (PI-IPS), the photoaligned IPS cell (CRM-IPS) exhibited an equivalent level of alignment state and electro-optical properties with outstanding anchoring stability and durability. Moreover, the cell showed an excellent dark state with a low light leakage due to the automatic compliance of optical axes. We demonstrated that the photo-induced alignment method based on the cinnamate-based reactive mesogen is a promising candidate for cost-effective, eco-friendly, and high-quality fabrication of high resolution LCDs.

Disclosure statement

No potential conflict of interest was reported by the authors.

Funding

ORCID

Myong-Hoon Lee ⓘ http://orcid.org/0000-0003-2505-1229

References

[1] Kim KH, Song JK. Technical evolution of liquid crystal displays. NPG Asia Mater. 2009;1:29–36.
[2] Schadt M, Seiberle H, Schuster A. Optical patterning of multi-domain liquid-crystal displays with wide viewing angles. Nature. 1996;381:212–215.
[3] Takeda A, Kataoka S, Sasaki T, et al. A super-high image quality multi-domain vertical alignment LCD by new rubbing-less technology. SID Int Symp Dig Tech Pap. 1998;29:1077–1080.
[4] Oh-e M, Kondo K. Electro-optical characteristics and switching behavior of the in-plane switching mode. Appl Phys Lett. 1995;67:3895–3897.
[5] Oh-e M, Kondo K. Response mechanism of nematic liquid crystals using the in-plane switching mode. Appl Phys Lett. 1996;69:623–625.
[6] Lee SH, Lee SL, Kim HY. Electro-optic characteristics and switching principle of a nematic liquid crystal cell controlled by fringe-field switching. Appl Phys Lett. 1998;73:2881–2883.
[7] Hong SH, Park IC, Kim HY, et al. Electro-optic characteristic of fringe-field switching mode depending on rubbing direction. Jpn J of Appl Phys. 2000;39:527–530.
[8] Yu IH, Song IS, Lee JY, et al. Intensifying the density of a horizontal electric field to improve light efficiency in a fringe-field switching liquid crystal display. J Phys D: Appl Phys. 2006;39:2367–2372.
[9] Ge Z, Wu ST, Kim SS, et al. Thin cell fringe-field-switching liquid crystal display with a chiral dopant. Appl Phys Lett. 2008;92:181109.
[10] Lyu JJ, Sohn JW, Kim HY, et al. Recent trends on patterned vertical alignment (PVA) and fringe-field

switching (FFS) liquid crystal displays for liquid crystal television applications. J Disp Technol. 2007;3:404–412.

[11] Yun HJ, Jo MH, Jang IW, et al. Achieving high light efficiency and fast response time in fringe field switching mode using a liquid crystal with negative dielectric anisotropy. Liq Cryst. 2012;39:1141–1148.

[12] Kim HY, Nam SH, Lee SH. Dynamic stability of the fringe-field switching liquid crystal cell depending on dielectric anisotropy of a liquid crystal. Jpn J Appl Phys. 2003;42:2752–2755.

[13] Park JW, Ahn YJ, Jung JH, et al. Liquid crystal display using combined fringe and in-plane electric fields. Appl Phys Lett. 2008;93:081103.

[14] Behdani M, Rastegar A, Keshmiri SH, et al. Submicron liquid crystal pixels on a nanopatterned indium tin oxide surface. Appl Phys Lett. 2002;80:4635–4637.

[15] Behdani M, Keshmiri SH, Soria S, et al. Alignment of liquid crystals with periodic submicron structures ablated in polymeric and indium tin oxide surfaces. Appl Phys Lett. 2003;82:2553–2555.

[16] Chaudhari P, Lacey J, Doyle J, et al. Atomic-beam alignment of inorganic materials for liquid-crystal displays. Nature. 2001;411:56–59.

[17] Doyle JP, Chaudhari P, Lacey JL, et al. Ion beam alignment for liquid crystal display fabrication. Nucl Instrum Methods Phys Res, Sect B. 2003;206:467–471.

[18] Ikeda T. Photomodulation of liquid crystal orientations for photonic applications. J Mater Chem. 2003;13:2037–2057.

[19] Ichimura K. Photoalignment of liquid-crystal systems. Chem Rev. 2000;100:1847–1874.

[20] Schadt M, Schmitt K, Kozinkov V, et al. Surface-induced parallel alignment of liquid crystals by linearly polymerized photopolymers. Jpn J Appl Phys. 1992;31:2155–2164.

[21] Haaren JV. Wiping out dirty displays. Nature. 2001;411:29–30.

[22] Hindmarsh P, Owen GJ, Kelly SM, et al. New coumarin polymers as non-contact alignment layers for liquid crystals. Mol Cryst Liq Cryst. 1999;332:439–446.

[23] Chaudhari P, Lacey JA, Lien SCA, et al. Atomic beam alignment of liquid crystals. Jpn J Appl Phys. 1998;37:55–56.

[24] Contoret AEA, Farrar SR, Jackson PO, et al. Polarized electroluminescence from an anisotropic nematic network on a non-contact photoalignment layer. Adv Mater. 2000;12:971–974.

[25] Komitov L, Ruslim C, Matsuzawa Y, et al. Photoinduced anchoring transitions in a nematic doped with azo dyes. Liq Cryst. 2000;27:1011–1016.

[26] Komitov L, Ichimura K, Strigazzi A. Light-induced anchoring transition in a 4,4′-disubstituted azobenzene nematic liquid crystal. Liq Cryst. 2000;27:51–55.

[27] Ruslim C, Ichimura K. Comparative studies on isomerization behavior and photocontrol of nematic liquid crystals using polymethacrylates with 3,3′- and 4,4′-dihexyloxyazobenzenes in side chains. Macromolecules. 1999;32:4254–4263.

[28] Chigrinov VG, Kozenkov VM, Kwok HS. Photoalignment of liquid crystalline materials. West Sussex: Wiley; 2008.

[29] Srivastava AK, Chigrinov VG, Kwok HS. Ferroelectric liquid crystals: excellent tool for modern displays and photonics. J Soc Info Disp. 2015;23:253–272.

[30] Fukuhara K, Nagano S, Hara M, et al. Free-surface molecular command systems for photoalignment of liquid crystalline materials. Nat Commun. 2014;5:3320.

[31] Ohtsuka K, Nagataki Y, Goda K, et al. Study of liquid crystal display fabricated using slit coater under two ultraviolet irradiation conditions. Jpn J Appl Phys. 2013;52:05DB4.

[32] Lee JM, Kim JH, Kim HJ, et al. Achieving a robust homogenously aligned liquid crystal layer with reactive mesogen for in-plane switching liquid crystal displays. Liq Cryst. 2017;44:1194–1200.

[33] Lin TC, Yu SC, Chen PS, et al. Fabrication of alignment layer free flexible liquid crystal cells using thermal nanoimprint lithography. Curr Appl Phys. 2009;9:610–612.

[34] Mizusaki M, Tsuchiya H, Minoura K. Fabrication of homogenously self-alignment fringe-field switching mode liquid crystal cell without using a conventional alignment layer. Liq Cryst. 2017;44:1394–1401.

[35] Olenik ID, Kim MW, Rastegar A, et al. Characterization of unidirectional photopolymerization in poly(vinyl cinnamate) by surface optical second-harmonic generation. Phys Rev E. 1999;60:3120–3128.

[36] Kim MW, Rastegar A, Olenik ID, et al. Alignment of nematic liquid crystals on an electrically poled photopolymer film. J Appl Phys. 2001;90:3332–3337.

[37] Jeong IH, Yu JH, Jin HS, et al. Novel approach to achieve conventional polyimide-less IPS/FFS LCDs. SID Int Symp Dig Tech Pap. 2014;45:1418–1420.

[38] Broer DJ, Boven J, Mol GN, et al. In-situ photopolymerization of oriented liquid-crystalline acrylates, 3†. Oriented polymer networks from a mesogenic diacrylate. Macromol Chem Phys. 1989;190:2255–2268.

[39] Lub J, Broer DJ, Hikmet RAM, et al. Synthesis and photopolymerization of cholesteric liquid crystalline diacrylates. Liq Cryst. 1995;18:319–326.